Predictive Simulation of Two-dimensional Flat Plate Boundary Layer Transition

Yunzhen Li*

Engineering, Dalian University of Technology & University of Leicester, Liaoning, China, 124000

ABSTRACT: The laminar-turbulent transition is an old but still not a fully solved problem, which is mainly studied from the following aspects: (1) how the perturbation is generated and the receptivity problems (2) linear and nonlinear problems during the evolution of the perturbation (3) numerical simulation of the transition problem and the actual prediction. Considering that the power system of the vehicle is working in a low Reynolds number environment for a long time when flying at high altitudes. In this article, the research focuses on the turbulence model with the introduction of the AGS transition model is used to simulate the two-dimensional flat plate boundary layer transition in the low Reynolds number case, and to predict the transition location by combining the stability of different positions of the flow process, and to evaluate the accuracy of the transition model in comparison with other numerical simulation methods.

1. INTRODUCTION

Laminar-to-turbulent flow transition is a widespread phenomenon in nature and various engineering practices. It was found that the properties of laminar and turbulent flows are very different. For example, as the Reynolds number changes, the surface frictional resistance in turbulent flow can be an order of magnitude greater than in laminar flow [1]. Therefore, for the design of aerospace, ships and vehicles, if we want to control the development of laminar flow and transition to reduce loss [2], we need to have a more comprehensive understanding of the development of surface boundary layer and a more accurate prediction of transition.

However, the accuracy of the existing models in predicting the flow field is not very satisfactory, one of the main reasons is that there is no general turbulence model with good prediction capability to accurately simulate the real complex flow inside the impeller [3]. Therefore, in order to make a more accurate prediction and simulation of complex phenomena such as transition and separation in the impeller blade surface boundary layer under low Reynolds number conditions, Yang, Zou et al. introduced the Abu-Ghannam and Shaw's transition model (AGS model) into the existing turbulence model to consider the transition phenomenon of the blade surface boundary layer at low Reynolds number [4]. Correspondingly, the predictive ability of the transition model is investigated by comparing it with numerical simulations such as the direct numerical simulation of transition (DNS) and the Reynolds averaging method (RANS). Furthering the application of the transitional models discussed in this paper to practical transitional prediction work, and this paper reveals that the AGS prediction model performs well in the prediction of laminar flow and transition process at low Reynolds number.

2. TYPE OF BOUNDARY LAYER TRANSITIONS

Boundary-layer transitions are nonlinear, multiscale, complex flow processes that have been studied as far back as the 19th century, with the Reynolds circular tube experiment in 1883 being the beginning of the study of flow transitions. Common boundary layer transitions can be classified into several categories, such as natural, bypass, and separated flow transition [5].

2.1. Natural transition

Natural transition usually occurs at turbulence levels less than 1% and are common in the external flow of subsonic vehicles. Schlichting provided an exhaustive description of the natural transition process (Figure 1) [6], which was divided into four characteristic stages: 1) Receptivity: After exceeding the critical momentum thickness Reynolds number, the small disturbance within the boundary layer destabilizes and begins to grow. 2) Linear region: The unstable T-S wave within the boundary layer follows the linear stability theory to go through a slow amplitude growth process. 3) Nonlinear region: When the unstable wave amplitude grows to a certain level, the three-dimensional nonlinear disturbance is generated in the form of secondary instability and the disturbance amplitude grows rapidly. 4) Laminar to turbulent breaking region: With the generation and aggregation of turbulence, the flow develops rapidly in transition to a turbulent state.

*Corresponding author. Email: Yl663@student.le.ac.uk

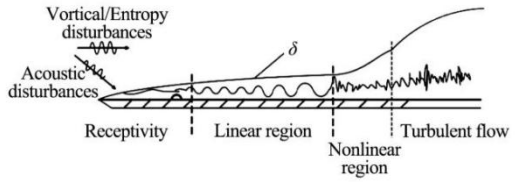

Figure 1 Natural transition process

2.2. Bypass transition

In flows where the incoming turbulence is greater than 1%, the sensory and linear phases of the natural turn are transgressed, and turbulent spots are generated directly in the boundary layer and develop rapidly into turbulence; this transition is known as the bypass translation.

2.3. separation flow transition

When the laminar boundary layer is separated by the reverse pressure gradient, the free shear layer is highly unstable due to the non-viscous instability mechanism, which makes transition very easy to occur.

3. TRANSITION FORECASTING METHOD

3.1. Direct numerical simulation method

Direct numerical simulation (DNS) can simulate the whole transition process from laminar to turbulent flow by solving the unsteady three-dimensional NS equation instead of Reynolds averaging. However, turbulence is an irregular multi-scale flow. In order to simulate full-scale vortices, high spatial and temporal resolution is required, and high computational capability is required, which makes it difficult to use this method directly in large-scale industrial simulation. In 1990, Gilbert and Kleiser used the time development method to simulate accurately the full transition from laminar to turbulent flow in a channel for the first time [7]. The calculation conditions were consistent with Nishika's experiments, with a Reynolds number of 5,000 and a vacancy grid distribution of 1,283. From the analysis of the results, Gilbert divided the turbulent turning process into three stages: (1) Increasing stage of initial disturbance; (2) Flow structure of transition from laminar to turbulent flow, such as formation and development stage of force vortices and high-shear layer; (3) Fracture stage. After three stages, there is fully developed turbulence. Figure 2 shows the laminar-turbulent transition in aerodynamics boundary layers. The three stages mentioned above correspond to $T \leq 100$, $100 < T \leq 150$ and $150 < T \leq 200$ respectively. In the third stage, the statistical mean value of the fluctuation and the average shear stress on the wall increase rapidly, and the disturbance can be significantly higher than the full development stage. After the flow has evolved into fully developed turbulence, the results are in agreement with those of Kim and Moyn [8].

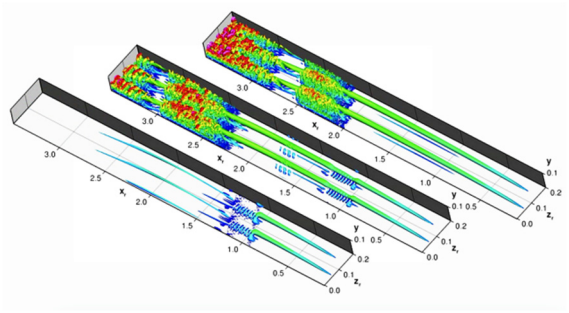

Figure 2 Laminar-Turbulent Transition in Aerodynamics Boundary Layers

The efficiency of solving flow field has always been a concern. A relatively successful algorithm is Newton iteration, which has a square convergence rate [9], which is much better than other standard linear convergence methods. There are basically three kinds of solutions for linear equations formed by Newton iteration: direct solution, iteration method and conjugate gradient method. The most attractive one is the conjugate gradient method. This method does not need to solve the inverse of the left-hand coefficient matrix, and only N steps are needed to get the solution of the equation (N is the number of equations) when solving it accurately. It not only saves memory but also has high efficiency. Among the common conjugate gradient methods, Sonneveld's Conjugate Gradient Squared (CGS) algorithm [10] and Saad and Schultz's Generalized Minimum RESidual (GMRES) algorithm [11] are more representative. etc.

3.2. Transition prediction by Reynolds averaging method

The Reynolds-averaging method approach to modelling turbulence captures the statistical properties of turbulent motion and is less demanding and has a shorter computational cycle time. The most commonly used modelling methods are the low Reynolds number turbulence model, the laminar flow energy model and the intermittency factor modelling. The low Reynolds number turbulence model was proposed by Jones and Launder [12] in 1973, which modelled the viscous sublayer with a damping function and directly modelled the flow state in the boundary layer. It was found that the decay function in the model equation could achieve the prediction of boundary layer transition, but the low Reynolds number turbulence model did not consider the physical mechanism of boundary layer transition, and the starting position of turning was advanced relative to the experimental results and the turning length was too short [13]. The Engineering Transition Model approach, which takes into account the intermittency factor, predicts the transition of the flow by introducing an intermittency factor transport equation, where the flow is laminar for an intermittency factor γ equal to 0 and turbulent for an intermittency factor γ equal to 1. Earlier, boundary layer transition prediction methods based on intermittent factor empirical relations were widely used, with the work of Dhawan and Narasirnha [14] being the most prominent, but such methods are somewhat empirical and not universally

applicable. Subsequently, Langtry proposed a $\gamma - \mathrm{Re}_{\theta t}$ transition model based on the $k-\omega$ SST turbulence model [15], which is based entirely on localized variables and can be coupled with existing massively parallelized CFD computational software and can accurately simulate and predict complex shaped boundary layer turning flows in three dimensions. In recent years, with the continuous development of computer computing power, some researchers [16] have started to carry out numerical calculations of boundary layer transition based on the hybrid RANS/LES method, in order to fully exploit the advantages of both the LES method and the RANS method, and to characterize the boundary layer transitional flow in a more detailed way while ensuring computational efficiency.

4. NUMERICAL SIMULATION

The calculation procedure is based on solving the two-dimensional constant Reynolds-averaged N-S equation using the finite volume method of spatial discretization, the time discrete implicit discretization method for the flow in AUSMDN format and the discrete linearized set of equations is solved using the GMRES algorithm. The turbulence model is a modified Spalart-Allmaras equation model.

4.1. Controlling equation

The controlling equation used in this paper is the two-dimensional constant Reynolds-averaged N-S equation derived from the Navier-Stokes (N-S) equation for incompressible fluids.

4.2. Discretization of the control equations

4.2.1. Spatial discretization

The spatial discretization of the control equations using the finite volume method becomes:

$$\frac{\mathrm{d}}{\mathrm{dt}}(\mathrm{U}\cdot\Omega)_{\mathrm{i}+\frac{1}{2},\mathrm{j}}+\left(\hat{\mathrm{F}}_{1+\frac{1}{2},\mathrm{j}}-\hat{\mathrm{F}}_{\mathrm{vi}+\frac{1}{2},\mathrm{j}}\right)-\left(\hat{\mathrm{F}}_{\mathrm{i}-\frac{1}{2},\mathrm{j}}-\hat{\mathrm{F}}_{\mathrm{vi}-\frac{1}{2},\mathrm{j}}\right) \quad (1)$$
$$+\left(\hat{\mathrm{G}}_{\mathrm{i,j}+\frac{1}{2}}-\hat{\mathrm{G}}_{\mathrm{vi,j}+\frac{1}{2}}\right)-\left(\hat{\mathrm{G}}_{\mathrm{i,j}-\frac{1}{2}}-\hat{\mathrm{G}}_{\mathrm{vi,j}-\frac{1}{2}}\right)=0$$

where U is the conservation variable, Ω is the area of the control cell, and 12 is the convective and diffusive fluxes in the direction of ζ, η in the generalized coordinate system, respectively. In this paper, the diffusive fluxes are discretized using the central difference, while the numerical convective fluxes are solved using Roe flux difference splitting (FDS) format [17].

$$\hat{\mathrm{F}}_{\mathrm{i}+\frac{1}{2},\mathrm{j}}=1/2[\hat{\mathrm{F}}(\mathrm{U_L})+\hat{\mathrm{F}}(\mathrm{U_R})-\left|\tilde{\mathrm{A}}(\mathrm{U_L},\mathrm{U_R})\right|\cdot(\mathrm{U_R}-\mathrm{U_L})] \quad (2)$$

Where,$\mathrm{U_L},\mathrm{U_R}$are the conservation variables on the left and right sides of the cell surface$(\mathrm{i}+1/2,\mathrm{j})$respectively; $\tilde{\mathrm{A}}(\mathrm{U_L},\mathrm{U_R})$ is the Roe averaged Jacobi coefficient matrix satisfying the U characteristic. In order to obtain spatially high order accuracy, the flow field variables on the left and right sides of the cell surface are obtained by the MuscL formula and the Van Albada limiter is used to prevent overshoot or over-expansion of the solution in the vicinity of the excitation wave. In addition, to satisfy the entropy condition, Hartan's entropy correction method was used [18].

4.2.2. Time discretization

Using the Euler posterior differential implicit time discretization method, equation (1) becomes:

$$\left(\frac{\Omega_{\mathrm{i,j}}}{\Delta\mathrm{t}}\mathrm{I}-\frac{\partial\hat{\mathrm{R}}^{\mathrm{n}}_{\mathrm{i,j}}}{\partial\mathrm{U}}\right)\cdot\delta\mathrm{U}=\hat{\mathrm{R}}^{\mathrm{n}}_{\mathrm{i,j}} \quad (3)$$

n represents the time layer, $\delta\mathrm{U}=\mathrm{U}^{\mathrm{n}+1}-\mathrm{U}^{\mathrm{n}}$, I is the unit matrix, $\hat{\mathrm{R}}$ is the residual vector.

$$\hat{\mathrm{R}}_{\mathrm{i,j}}=-\left(\hat{\mathrm{F}}_{\mathrm{i}+\frac{1}{2},\mathrm{j}}-\hat{\mathrm{F}}_{\mathrm{vi}+\frac{1}{2},\mathrm{j}}\right)+\left(\hat{\mathrm{F}}_{\mathrm{i}-\frac{1}{2},\mathrm{j}}-\hat{\mathrm{F}}_{\mathrm{vi}-\frac{1}{2},\mathrm{j}}\right)-\left(\hat{\mathrm{G}}_{\mathrm{i,j}+\frac{1}{2}}-\hat{\mathrm{G}}_{\mathrm{vi,j}+\frac{1}{2}}\right)+\left(\hat{\mathrm{G}}_{\mathrm{i,j}-\frac{1}{2}}-\hat{\mathrm{G}}_{\mathrm{vi,j}-\frac{1}{2}}\right) \quad (4)$$

The Jacobi matrix with respect to the residual vector can be written as:

$$\frac{\partial\hat{\mathrm{R}}^{\mathrm{n}}_{\mathrm{i,j}}}{\partial\mathrm{U}}=-\frac{\partial(\hat{\mathrm{F}}^{\mathrm{n}}_{\mathrm{i}+\frac{1}{2},\mathrm{j}}-(\hat{\mathrm{F}}^{\mathrm{n}}_{\mathrm{vi}+\frac{1}{2},\mathrm{j}})}{\partial\mathrm{U}}+\frac{\partial(\hat{\mathrm{F}}^{\mathrm{n}}_{\mathrm{i}-\frac{1}{2},\mathrm{j}}-(\hat{\mathrm{F}}^{\mathrm{n}}_{\mathrm{vi}-\frac{1}{2},\mathrm{j}})}{\partial\mathrm{U}}-\frac{\partial(\hat{\mathrm{F}}^{\mathrm{n}}_{\mathrm{i,j}+\frac{1}{2}}-(\hat{\mathrm{F}}^{\mathrm{n}}_{\mathrm{vi,j}+\frac{1}{2}})}{\partial\mathrm{U}}+\frac{\partial(\hat{\mathrm{F}}^{\mathrm{n}}_{\mathrm{i,j}-\frac{1}{2}}-(\hat{\mathrm{F}}^{\mathrm{n}}_{\mathrm{vi,j}-\frac{1}{2}})}{\partial\mathrm{U}} \quad (5)$$

Writing the control equations for each control unit as in equation (3), and combining all the control equations together, gives the following matrix equation system form:

$$\mathrm{A}\cdot\mathrm{X}=\mathrm{B} \quad (6)$$

where A is an N x N coefficient matrix, and N is the number of control units in the computational domain. For two-dimensional problems, each element of the matrix A is a matrix of order 4 x 4.

x is the solution vector $\{\delta\mathrm{U}_1,\delta\mathrm{U}_2\ldots\ldots\delta\mathrm{U}_{\mathrm{n}-1},\delta\mathrm{U}_{\mathrm{n}}\}$ and B is the residual vector for each time step, the coefficient matrix at the left end of equation (3) and the residual vector at the right end are known, i.e. both A and B are known, so the system of equations (6) becomes a linear system.

4.3. Introduction of the AGS transition model

The computational procedure is based on solving the two-dimensional Reynolds-averaged N-S equations using the finite volume method for spatial discretization, the implicit discretization method for temporal discretization, the AUSMDN format for the circulation and the GMKES algorithm for the discrete set of linearized equations. The turbulence model is a modified Spalart-Allmaras equation model [19].

The turbulent viscosity is modified by the AGS transition model to account for the turning process as follows:

$$\mu_{\mathrm{eff}}=\mu_{\mathrm{lam}}+\mu_{\mathrm{turb}} \quad (7)$$

$$\begin{cases}\gamma=0 & \text{laminar zone}\\ \gamma=1-\exp(-5\eta^3) & \text{transition zone}\\ \gamma=1 & \text{turbulent zone}\end{cases} \quad (8)$$

$$\eta=\frac{\mathrm{X}-\mathrm{X_s}}{\mathrm{X_E}-\mathrm{X_s}} \quad (9)$$

where γ is defined as the interval factor, η is a dimensionless constant indicating the length parameter. In equation (9), $\mathrm{X},\mathrm{X_s},\mathrm{X_E}$ is the arc length from the leading

edge at a point in the transition zone, at the start of the turn, and at the end of the turn, respectively.

The momentum thickness Reynolds number is applied to predict the start of a turn, and when the momentum thickness Reynolds number reaches a critical Reynolds number, the turn is considered to have occurred. The critical Reynolds number is defined as:

$$\mathrm{Re}_{\theta s} = \exp\left\{F(\lambda_\theta) - \frac{F(\lambda_\theta)}{6.91}\tau\right\} + 163. \quad (10)$$

The range of $F(\lambda_\theta)$ in the equation is:

$$F(\lambda_\theta) = 6.91 + 12.57\lambda_\theta + 63.34{\lambda_\theta}^2 \quad (\lambda_\theta < 0) \quad (11)$$

$$F(\lambda_\theta) = 6.91 + 2.48\lambda_\theta - 12.27(\lambda_\theta)^2 \quad (\lambda_\theta > 0) \quad (12)$$

λ_θ is the Thwaites pressure gradient parameter which defined as:

$$\lambda_\theta = \left(\frac{\theta^2}{v}\right)\left(\frac{dU_\infty}{dx}\right) \quad (13)$$

R_L is the transition length Reynolds number,

$$R_L = 16.8(R_{XS})^{0.8} \quad (14)$$

$$R_{XS} = \frac{X_S U_{\infty S}}{v} \quad (15)$$

R_{XS} is the Reynolds number at the beginning of the transition.

Yang et al. used a BL function approach based on the Ba|dwin - Lomax model to calculate the momentum thickness of the boundary layer.

According to the BL function equation:

$$f(y) = y|\omega|(1 - e^{-\frac{y^+}{A^+}}) \quad (16)$$

Where $A^+ = 26$, ω is the vortex, y is the distance to the wall.

A distribution of $f(y)$ is obtained in the normal direction of the wall, where the maximum value of $f(y)$ is f_{max}, and look for the position of $f(y) = {}^1/_2 f_{max}$ at that point in the direction away from the wall, where y is y_{half}, then we consider the edge of the boundary layer is:

$$\delta = {}^1/_2 y_{half} \quad (17)$$

The momentum thickness of the boundary layer is obtained by integrating along the normal direction.

$$\theta = \int_0^\delta \frac{\rho u}{\rho_e u_e}(1 - \frac{u}{u_e})dy \quad (18)$$

5. CALCULATION RESULTS

5.1. 2D flat-panel computing

Applying the results of the AGS transition model above, the results of the analysis of the two-dimensional flat plate are presented in the form of a software simulation with 61 and 101 grid points in the spreading and flow directions respectively, and the grid is encrypted near the wall to capture the variation in velocity distribution in the boundary layer. The flow direction is also gridded more densely in order to better determine the location of the start and end points of the turn. The Reynolds number based on the plate length in the calculation is 1.8×10^6.

Figure 3 shows the development of the Reynolds number for the boundary layer momentum thickness, figure 4 shows the distribution of the frictional drag coefficient at the wall along the flow direction.

The experimental values indicated by the dots in the figure are the results obtained by Abu Ghannam and Shaw [20]. The solid line is the result of introducing the transition model, while the dashed line is the result of using the SA turbulence model [19] without the transition model.

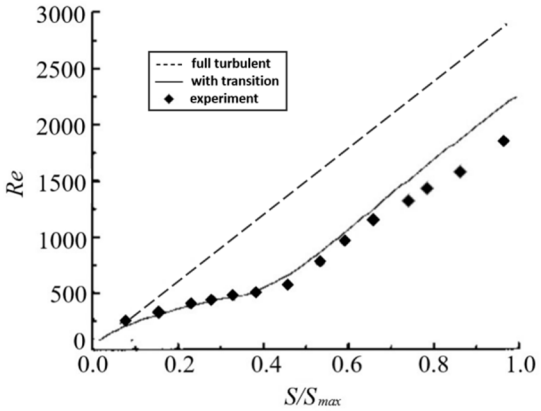

Figure 3 Development of momentum thickness Reynolds number of boundary layer

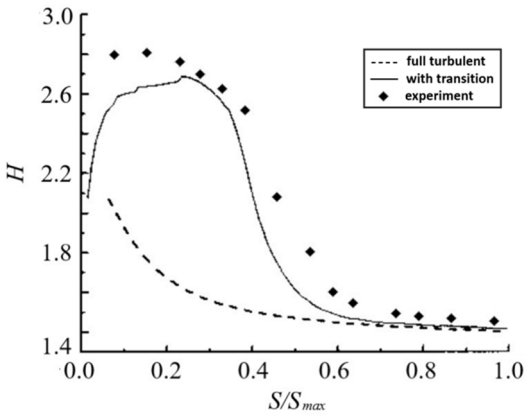

Figure 4 Wall friction coefficient distribution

Comparing the predictions of other turbulence models, Yang Jinlong et al. give the prediction of the wall friction drag by a transition model based on time-averaged Reynolds simulations [21].

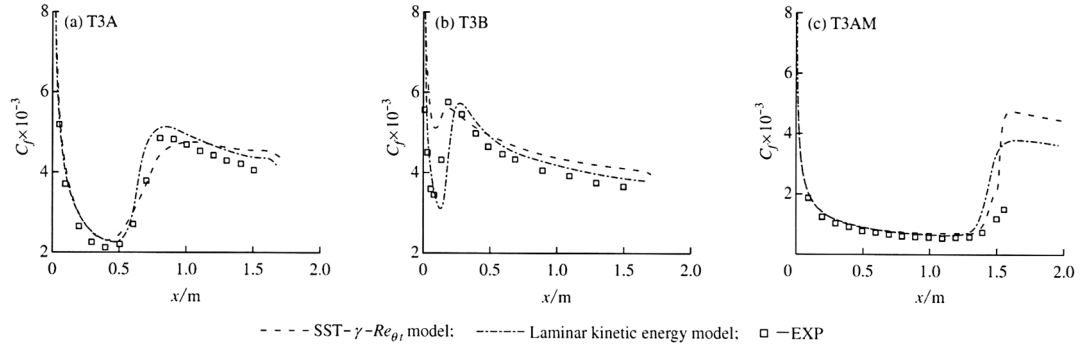

Figure 5 Skin friction coefficient of zero pressure gradient

A comparison of the experimental results shows that the development of friction at the two-dimensional flat plate wall under a zero-pressure gradient based on time-averaged Reynolds simulations at moderate turbulence is not very different from that predicted by the introduction of the AGS transition model, both capturing the start and development of the transition process more accurately, and the obtained boundary layer parameters are in better agreement with the experimental values. The simulated AGS model for the zero-pressure gradient flat plate boundary layer gives a slightly earlier estimate of the start and end of the transition.

5.2. Simulation of the presence of pressure gradients

The flat plate example with pressure gradient focuses on the effect of pressure gradient on the prediction of the transition model. The experimental model is similar to the non-pressure plate experiment, except that the upper wall surface is a contracted/expanded surface. Compared to the average Reynolds simulation model of Yang Jinlong et al. which predicts the transition in the presence of pressure gradients relatively completely [21], the transition prediction model with AGS in the presence of pressure gradients and curvature in the boundary layer needs to be further modified to determine the transition onset. The problem of delay in the prediction of the transition point relative to the actual value of the model is solved.

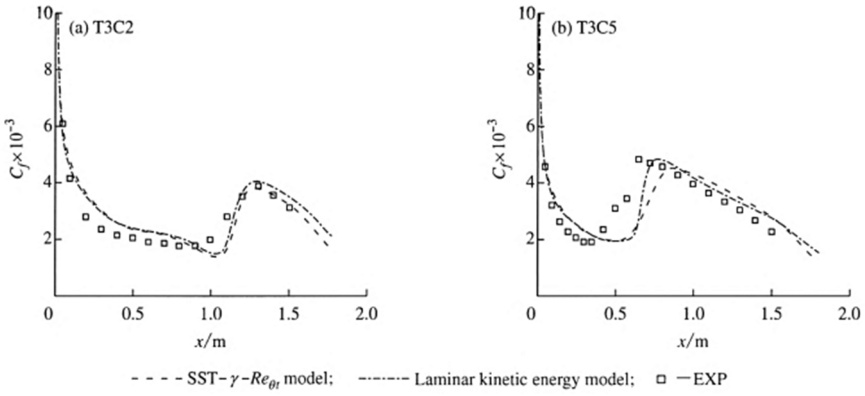

Figure 6 Skin friction of non-zero-pressure-gradient cases

6. CONCLUSION

The main work of this paper is to introduce the Abu-Ghannam and Shaw's transition Model (AGS model) into the existing turbulence model in numerical simulations. to the existing turbulence model in order to consider the transition of the blade surface boundary layer at low Reynolds numbers. The article compares the results of the time-averaged Reynolds simulations with the turbulence model with the introduction of the AGS transitional model of flat plate boundary layer transition and concludes that its accuracy and applicability can be improved in some specific cases. Future improvements and applications of the model in practical engineering will be pursued.

1. The numerical method of Reynolds averaging performs well in predicting laminar and turbulent processes at low Reynolds numbers but needs to be further investigated in conjunction with different turbulence and turbulence models.

2. The AGS transitional model can predict the onset and progression of transitions more accurately to reflect the development of the boundary layer under low Reynolds number conditions.

3. In the presence of pressure gradients and curvature in the boundary layer, the criterion for determining the starting point of the transition needs further revision.

4. The future development of the prediction model can consider the combination of multiple models, so that the model can reveal the physical mechanism of boundary transition more comprehensively and provide an efficient numerical calculation tool for the study of boundary layer transitions.

REFERENCES

1. Gad—el-HaL Flow Contr01. Cambridge: The University of Cambridge, 2000, 104~105
2. Lake J, King P, Rivir R. Reduction of separation losses on a turbine blade with low Reynolds numbers[C] // Aerospace Sciences Meeting & Exhibit. 2013.
3. Bradshaw P. Turbulence modeling with application to turbomachinery[J]. Progress in Aerospace Sciences, 1996.
4. Yang Lin, Zou Zhengping, Ning Fangfei, et al Numerical simulation of boundary layer transition [J] Journal of Aeronautical power, 2005, 20 (3): 6
5. Mayle R. The role of laminar-turbulenttransition in gas turbine engines[C]. 1991.
6. Schlichting H, Gersten K, Krause E, eta1. Boundary—layer theory[M]. Springer, 1955.
7. Gilbert, N. Kleiser, L. 1990, Near-wall phenomena in transition to turbulence. In near-wall turbulence: 1988 Zoran Zaric Wea Conf., Ed S.J. Kline, N.H. Afgan, pp7—27, Washington, DC: Hemisphere.
8. Kim J, Moin P, Moser RD. 1987. Turbulence statistics in fully - developed channel flow at low Reynolds number. J. Fluid Mech 177: 133—66
9. Orkwis PD, George JH. A comparison of CGSP preconditioning methods for Newton's method solvers. AIAA Paper, 9-33327, 1993
10. Sonneveld P.CGS, A fast Lanczos-type solver for nonlinear systems. SIAM Journal of scientific statistics and computing, 1987, 10; 350-356
11. Saad Y, Schultz MH. GMRES, A generalized minimal residual algorithm for solving nonsymmetric linear systems. SIAM Journal of scientific statistics and computing, 1986, 7; 856-869
12. Jones W P, Launder B. The calculation of low-Reynolds—number phenomena with a two—equation model of turbulence[J]. International Journal of Heat and Mass Transfer. 1973, 16(6): 1119-1130.
13. Schmidt R C, Patankar S V Two-Equation Low-Reynolds. Number Turbulence Modeling of Transitional Boundary Layer Flows Characteristic of Gas Turbine Blades. Ph.D. Thesis. Final Contractor Report[J]. 1988.
14. Dhawan S J, Narasimha R. Some properties of boundary layer flow during the transition from laminar to turbulent motion [J], Journal of Fluid Mechanics. 1958, 3(4): 418, 436.
15. Malan P, Suluksna K, Juntasaro E. Calibrating the y-Re0 transition model for colmnercial CFD[C]. 2009.
16. You J Y, Kwon O J, Blending of SAS and correlation—based transition models for flow simulation at supercritical Reynolds numbers [J]. Computers & Fluids. 2013, 80: 63—70.
17. Roe PL. Approximate Riemann solver, parameter vector, and difference schemes. Journal of Computational Physics. 1981,433; 357-372.
18. Ning Fangfei, Xu Liping GMRES algorithm in two-dimensional steady turbulence calculation [J] Journal of mechanics, 2001 (04): 442-451
19. Ning, F., and L. Xu. "Numerical Investigation of Transonic Compressor Rotor Flow Using an Implicit 3D Flow Solver with One-Equation Spalart-Allmaras Turbulence Model." Asme Turbo Expo: Power for Land, Sea, & Air 2001.
20. BJ Abu-Ghannam, and R Shaw. "Natural Transition of Boundary Layers—The Effects of Turbulence, Pressure Gradient, and Flow History." Journal of Mechanical Engineering Science (2006).
21. Yang Jinlong, Two transition models for Reynolds time averaged simulation and flow prediction [D] East China University of technology, 2014